Synthesis and Characterization of Congeners of Misonidazole for Imaging Hypoxia

Zdenka Grunbaum, Sara J. Freauff, Kenneth A. Krohn, D. Scott Wilbur, Sara Magee, and Janet S. Rasey

Departments of Radiology and Radiation Oncology, University of Washington, Seattle; School of Medicine, University of California, Davis; and NeoRx Corporation, Seattle, Washington

Misonidazole is a known hypoxic cell sensitizer that binds covalently in hypoxic cells. Its congeners labeled with [77]Br, [75]Br, or ^{18}F, are likely candidates for imaging hypoxia. We have synthesized and tested [[82]Br]-4-bromomisonidazole, [^{3}H]-4-bromomisonidazole, [^{3}H]fluoromisonidazole and [^{3}H]misonidazole as prototype radiopharmaceuticals and have compared their uptake in normal and malignant tissues. The higher lipophilicity of brominated misonidazole increased its concentration in the hypoxic portion of tumors at 2 hr, but high blood levels contributed to excessive background, incompatible with imaging. Hydrogen-3-fluoromisonidazole diffused into tumors at a slower rate than misonidazole but it also cleared from normal tissues so that after 2 hr tumor-to-blood ratios favorable for imaging were achieved. In the compounds that were studied, fluorine at the end of the alkyl chain is more stable in vivo than bromine on the imidazole ring. Our results indicate that [^{18}F] fluoromisonidazole may be a useful tracer for imaging hypoxia at ~4 hr after injection.

Our laboratory has been working to develop tracers whose biodistribution would reflect intracellular oxygen concentration. Specifically, we seek tracers that will localize within cells in inverse proportion to their oxygen content so that hypoxia can be imaged with positron emission tomography (PET) or single photon emission computed tomography (SPECT) as an intense concentration of radioactivity. Such tracers may provide a better defined image than possible with $O^{15}O$ and measurements of rMRO₂, the regional metabolic rate for O_2.

This proposed tracer should initially distribute non-selectively throughout all tissues, reaching an early equilibrium distribution that is proportional to its partition coefficient in each tissue. An intracellular reaction would then occur at a rate inversely proportional to the intracellular oxygen concentration, to retain the tracer in tissues. Any tracer that was not trapped by this reaction would wash out, resulting in the desired positive image of hypoxic tissues. The nitroimidazole radiosensitizers, typified by misonidazole, exhibit these characteristics. Misonidazole exhibits three properties in hypoxic cells: sensitization to ionizing radiation, direct cytotoxicity, and covalent binding (1). The latter property forms the basis for imaging.

The early biodistribution of labeled misonidazole is influenced principally by the drug's partition coefficient since nitroimidazoles penetrate lipid membranes by passive diffusion, the rate increasing with lipophilicity (2). Nitroimidazoles of the same electron affinity but different partition coefficients produce peak concentrations in tumors that are positively correlated with their lipophilicity (3,4). There will be an optimal partition coefficient for our proposed hypoxia imaging agent.

Several radiolabels for misonidazole were considered. We rejected nitrogen-13 and carbon-11 because their half-lives are too short for the required sequence of biologic events that would lead to the proposed image. The two most promising approaches appeared to be halogenation on the ring or at the end of the alkyl chain. Preliminary research using tritium-, carbon-14-, and bromine-82- ([82]Br) labeled derivatives of misonidazole has explored the feasibility of imaging hypoxic tissues in tumors (5–7) or ischemia in nonmalignant tissue (8–11). Previous studies by our group have shown that 4-bromomisonidazole uptake in hypoxic tissue is equal or greater than that of tritiated misonidazole. This paper reports on high yield syntheses of labeled misonidazole congeners and studies of their metabolism and their biodistribution in vivo.
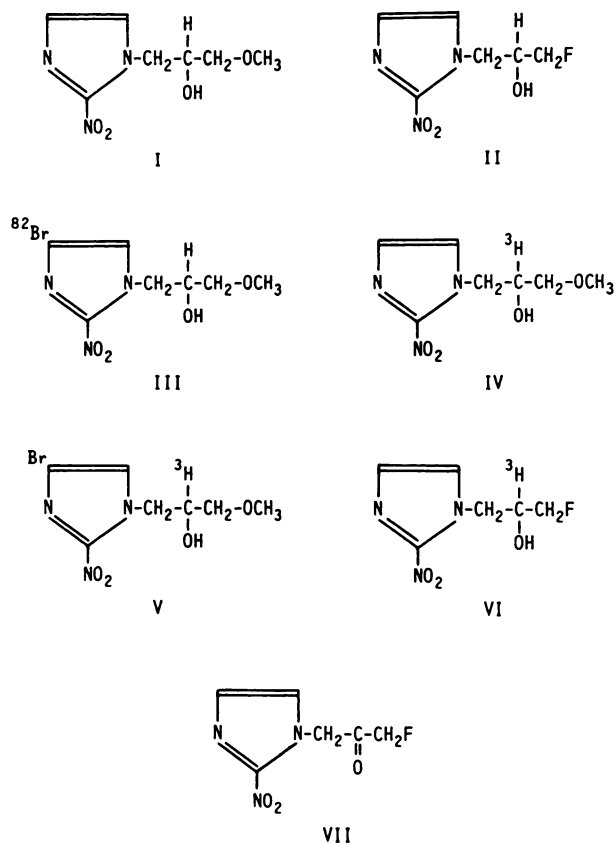
FIGURE 1

Chemical structures: (I) misonidazole; (II) fluoromisonidazole; (III) [^{82}Br]-4-bromomisonidazole; (IV) [^{3}H]misonidazole; (V) [^{3}H]-4-bromomisonidazole; (VI) [^{3}H]fluoromisonidazole; (VII) ketone derived from fluoromisonidazole.

MATERIALS AND METHODS

Misonidazole (*I*) and fluoromisonidazole (*II*) (Fig. 1) were recrystallized to a constant melting point prior to use. Compounds (III–IV) were synthesized in our laboratories as described in the section on syntheses. All other chemicals were of reagent quality or better and were obtained from commercial sources. All solvents used were of high performance liquid chromatography (HPLC) grade.

Chromatography

Analytical reverse phase HPLC* was used for monitoring the progress of reactions, determining radiochemical purity of products, and identifying the metabolites in biological fluids and tissue extracts. A C-18 column (10 μ, 25 × 0.4 cm) was used at a flow rate of 1 ml/min and the eluent was monitored at 340 nm. The pumps were used in the isocratic mode or with a linear gradient.

Sephadex G-10-120 preparative chromatography (40–120 mesh, 1.5 × 70 cm column) was used to isolate products from the reaction mixture. In this separation, the dextran polymer functioned as a weak ion exchanger. The eluent was double-distilled water at a flow rate of 13 ml/hr. Retention times for misonidazole and 4-bromomisonidazole were measured prior to each radiolabeling experiment to compensate for changes in the flow or settling of the Sephadex. Ultraviolet (uv) absorbance spectra of the fractions were compared with those of standards. The retention volumes of the major products of the bromination of misonidazole are given in Table 1.

The samples of kidney, liver, and plasma described in the later section on biologic methods were analyzed by HPLC using a C-18 column. The mobile phase was a linear acetonitrile/water gradient (15–60%). The column eluent was monitored by a flow-through uv detector at 340 nm and eluent at the appropriate retention volumes was collected to be counted. Table 1 gives retention volumes for parent compounds and metabolites.

The ^{82}Br-labeled products were assayed in a gamma well or a dose calibrator. Biologic fluids and tissue samples were counted in a gamma spectrometer† with multichannel analysis capability. The HPLC fractions labeled with tritium were counted in a liquid scintillation spectrometer in Instagel scintillation fluid‡ and efficiencies were calculated from a standard curve determined with a series of quenched tritium standards. The samples were counted to 1% error.

Characterization of Products

Proton nuclear magnetic resonance spectra were obtained using a Nicolet 500 MHz spectrometer operated in Fourier Transform mode. Sodium 2,2-dimethyl-2-silapentane-5-sulfonate (DSS) dissolved in D$_2$O was used as the internal standard in each spectrum. Ultraviolet absorbance of the compounds at 340 nm was measured using a uv-visible spectrophotometer§ operated with a rapid sampler and peak chromatographic fractions were scanned between 215 and 380 nm to determine lambda$_{max}$ (λ) and their molar extinction coefficients (ϵ). Octanol/water partition coefficients were determined by the method of Fujita (*12*), using optical density to quantitate concentration of unlabeled drug or gamma-ray detection to measure concentration of radiolabeled compounds.

TABLE 1
Physical Parameters of Misonidazole and Congeners

| | Retention volumes | | uv Absorbtion | |
	Preparative (ml)	Analytical (ml)	Lambda$_{max}$ (nm)	Ext. coeff. (liter·cm^{-1} mole^{-1})
Br$^-$	75–83	2.8–3.2	—	—
Misonidazole	114–115	9.6–10.0	325	7.5 × 10^3
4-Bromomisonidazole	180–185	17.6–18.0	340	7.73 × 10^3
5-Bromomisonidazole	145–145	—	—	—
Desmethylmisonidazole	—	4.0–4.4	—	—
Desmethyl-4-Br-misonidazole	—	4.0–4.4	—	—
Fluoromisonidazole	—	8.8–9.2	324	7.72 × 10^3

Synthesis of [⁸²Br]-4-Bromomisonidazole (III)

The synthesis of (III) based on the exchange of molecular bromine with anhydrous $NH_4{}^{82}Br$ was described previously (6). An alternate synthesis of (III) of higher specific activity was achieved by generating a brominating agent in situ (13) using anhydrous $K^{82}Br$ (9.8 mCi, 3 mCi/mg bromide, 4.2 × 10^{-2} mmole)¹ and N-chlorosuccinimide. The glass ampule containing the radioactive material was crushed in a 5 ml reaction flask, 0.5 ml absolute methanol was added, and the mixture was stirred until all KBr dissolved. After addition of 8.5 mg misonidazole (4.2 × 10^{-2} mmol), the mixture was stirred and then warmed to 45°C to assist the dissolution of reagents (30 min). The bromination was initiated by adding 11.2 mg of N-chlorosuccinimide (8.4 × 10^{-2} mmol) directly as a solid. The reaction mixture was stirred for 5 min at room temperature and then heated to 45°C for 3 hr. The progress of the reaction was monitored by HPLC using the analysis described above. The reaction mixture was then rotary evaporated to dryness, dissolved in 1.5 ml water and purified by preparative chromatography.

Synthesis of [³H]-4-Bromomisonidazole (V)

Compound (V) (Fig. 1) was synthesized by bromination of (IV) as previously described (7,14).

Synthesis of [³H]Fluoromisonidazole (VI)

Fluoromisonidazole (II) was oxidized by CrO_3/H_2SO_4 (15) to yield ketone (VII). Compound (II) (250 mg, 1.32 mmol) was dissolved in 6.3 ml acetone at room temperature. Freshly prepared CrO_3/H_2SO_4 (4.3 mmol/ml) was added dropwise with stirring. At the beginning of reaction 0.3 ml was added and this was supplemented at 20 and 35 min with aliquots of 0.2 ml each. Following each aliquot the mixture was stirred and warmed on a water bath to 25-28°C. After the addition of the last aliquot the mixture was stirred for 2 hr, cooled in an ice bath, and 0.63 ml distilled water added to destroy excess chromium oxide reagent. The reaction mixture was kept at 4°C and concentrated ammonia was added dropwise to attain a pH of 5. The reaction mixture was then filtered and the filtrate was extracted repeatedly (25, 12, and 12 ml) with ethyl acetate. The wash solutions were combined and dried with anhydrous $MgSO_4$, filtered, and the solvent removed by rotary evaporation. The product mixture was ground with ether in a mortar to extract the ketone and the ether solution filtered and then evaporated in vacuum. The crude ketone (VII), recrystallized twice from benzene and dried in vacuum, had a melting point of 77°C.

The reduction of 1-(3-fluoro-2-oxopropyl-2-nitro-1H-imid-azole (VII) was accomplished using tritiated $NaBH_4$. A sample of 8 mg of (VII) (0.04 mmol) was dissolved in 0.15 ml of absolute ethanol under nitrogen and warmed to 35°C to achieve complete solution. The glass ampule containing the reducing agent, [³H]-$NaBH_4$ (0.01 mmol, 294 mCi/mg),** was opened under nitrogen and the solution of (VII) added. The sides of the ampule were washed with an additional 0.1 ml of absolute ethanol and the reaction mixture was stirred in a glove box for 2.5 hr at room temperature. At the end of the reaction the mixture was filtered through a glass wool plug into a tube containing 100 mg of carrier fluoromisonidazole. The tube was warmed on a water bath until total dissolution occurred, and the cooled crystals were filtered and recrystal-lized twice. Radiochemical purity was determined by HPLC.

Biological Evaluation: Mouse and Tumor System

Four tracer compounds, (III), (IV), (V), and (VI), were evaluated in tumor bearing mice to determine their biodistri-bution in malignant and normal tissues, and their stability in vivo. For studies with radiolabeled misonidazole or bromo-misonidazole female BALB/c Km mice were injected subcu-taneously with EMT6/UW cells (16). At ~12 days after implant the tumors were 50-200 mm³. Additional studies with (IV) and all investigations with (VI) used C3H/km mice bearing KHT tumors (17). Tumors were used for experiments when they reached 50-200 mm³, at 8-11 days after transplant. The KHT tumor is a more consistent tumor line and the C3H mice used in the later experiments were the same weight as the BALB/c's (25-28 g). Distribution for nonmalignant tissues (% ID/g) was the same for the two strains of mice injected with misonidazole.

The mice were injected intraperitoneally with radioactive drug plus carrier drug in normal saline at a concentration of 1.4 mg/ml to achieve an injected dose of 50 μmol/kg. Each mouse received 4.7 × 10^7 dpm ⁸²Br and 7.3 × 10^6 dpm of tritium. In parallel experiments with (IV) each mouse received a 50 μmol/kg dose with 4 × 10^7 dpm of tritium. The quantity injected was measured by weighing the injection syringe and a standard aliquot was counted to calculate the total injected dose. Previous studies have shown similar plasma and tumor levels in mice injected intraperitoneally or intravenously with misonidazole or congeners (3,6,18).

Blood samples were taken at 5, 15, 30, 60, and 120 min after injection. Each mouse provided three blood samples, two by heparinized capillary from the retroorbital plexus and one from the brachial plexus upon death. The mice were killed at 120 min and tissue samples were taken from tumor, liver, kidney, heart, brain, and lung. The samples were weighed and gamma counted for ⁸²Br. The ⁸²Br was then allowed to decay to background and the tissues were solubilized and analyzed for tritium. Percent injected dose per gram, % ID/g was calculated for each tissue. The uptake of (IV) into eight different tissues of mice from the two strains was statistically equivalent, as was the fraction of radiobiologically hypoxic cells in the two tumors (30%). The proportion of hypoxic cells is defined operationally as the percentage of cells at $O_2 \leq 1,000$ ppm and are therefore threefold as resistant to cytotoxic effects of ionizing radiation as are fully oxygenated cells. This is determined by analysis of the radiation cell survival curves for mouse tumors irradiated in air breathing and N_2 asphyxiated animals (19), an established procedure in radiation biology. We thus concluded that intercomparison of different drugs between two different mouse strains was justified.

HPLC separated the 4-bromomisonidazole metabolites in plasma and tissues of mice receiving i.p. injection of 50 μmol/kg of radiochemically pure, radiolabeled drug, ~4.7 × 10^8 dpm of ⁸²Br and 7.3 × 10^7 dpm of tritium. The mice were killed at 15, 30, or 120 min. Liver and kidney were quick frozen in liquid nitrogen and stored at −70°C. Blood clearance was measured with samples taken at 5, 15, 30, 60, and 120 min. Heparinized plasma samples were obtained by spinning whole blood. Hematocrits were also measured at 15, 30, and 120 min and were used in the calculation of a partition coefficient between blood cells and plasma. The samples of whole blood and plasma were counted for radioactivity and the ratio of the activities of equal volume was calculated using specific densities (20).

TABLE 2
Effect of Substitution on Lipophilicity of Misonidazole Congeners

Compound	Partition coefficient
Misonidazole	0.41
4-Bromomisonidazole	2.87
5-Bromomisonidazole	1.46
4,5-Dibromomisonidazole	10.53
Fluoromisonidazole	0.40

activities of equal volume was calculated using specific densities (20).

Plasma samples were prepared for HPLC by first deproteinizing with 1:3 acetonitrile/methanol (21), vortexing, centrifuging, and washing the precipitate. The combined supernatant and washes were concentrated under a gentle stream of nitrogen and assayed for metabolites by HPLC. Quick frozen liver and kidney samples were processed similarly.

RESULTS

The two approaches to bromination of misonidazole varied in yields and in ease of purification of the 4-bromomisonidazole product. Direct bromination using Br_2 resulted in low yields of 4-bromomisonidazole (23%) and a substantial amount of the 5-bromo isomer (15%). Separation of the two positional isomers from the other reaction products by Sephadex required, in some cases, rechromatographing the peak fractions, with resultant loss of product. The eluted fractions of [^{82}Br]-4-bromoisonidazole obtained from the reaction of N-chlorosuccinimide and $K^{82}Br$ contained >75% of the bound radioactive bromine. A sample of [^{82}Br]-4-bromoisonidazole rechromatographed by analytical

HPLC showed radiochemical purity was equal or better than 99%.

Assignment of structure for the two mono-brominated misonidazoles was based on the chemical shifts of proton resonances in the alkyl chain of the molecules. Bromination at the more distant 4-position of the imidazole ring would be expected to produce the smallest effect on the aliphatic protons adjacent to the ring. The proton resonances assigned to 4-bromomisonidazole are virtually unchanged from those of misonidazole, except for the aromatic proton at the ring-5 position which shows an expected downfield shift from 7.44 to 7.53 ppm. Bromination at the ring-5 position also produced downfield shifts in 5-bromomisonidazole (from 7.19 to 7.32 ppm). However, the magnitude of the shift was not equal for the protons of the side chain next to the ring; in the protons next to the methoxy group it was virtually unchanged in all three compounds. Little, if any, effect might be expected on the methyl protons of the methoxy group because of their distance from the ring. Hindered rotation may account for the nonequivalent nature of quartets for the four methylene protons.

The two halogenated misonidazoles have the uv characteristics shown in Table 1. The octanol-water partition coefficients of misonidazole and its halogenated congeners were measured and the effect of bromination on lipophilicity of misonidazole is shown in Table 2.

The blood clearance curve of [^3H]-4-bromomisonidazole (V) administered intraperitoneally in mice demonstrated two phases (Fig. 2). The faster component cleared with a half-life of 30 min, while the slower had a half-life of over 70 min and resulted in relatively high blood levels over the first 2 hr. [^{82}Br]-4-bromomisonidazole (III) cleared more slowly than its tritium analog
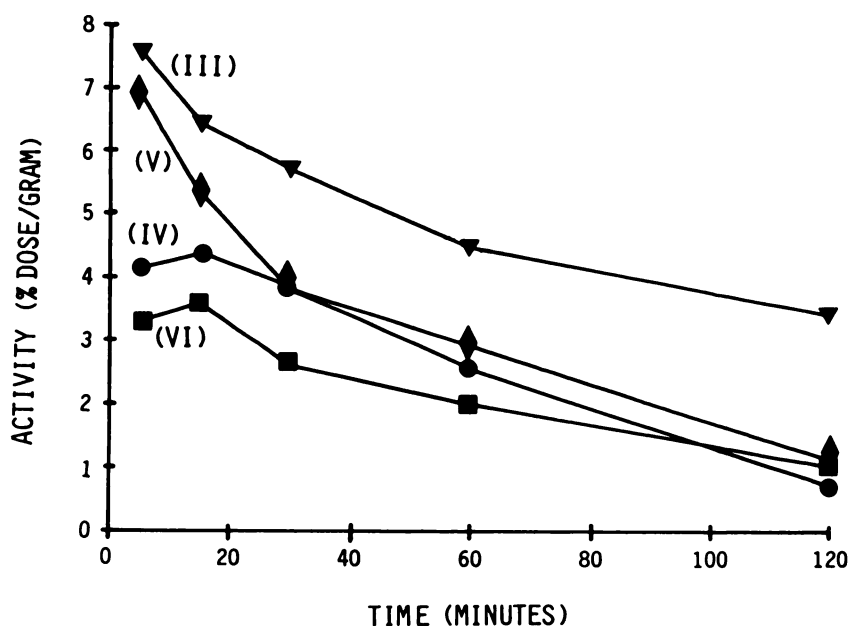

FIGURE 2
Blood clearance curves: (III) [^{82}Br]-4-bromomisonidazole; (IV) [^3H]misonidazole; (V) [^3H]-4-bromomisonidazole; (VI) [^3H]fluoromisonidazole.

TABLE 3
Tissue Uptake at 2 hr

	% Injected dose/g tissue			
Tissue	[^{82}Br]-4-bromo-misonidazole* (n = 5)	[^{3}H]-4-bromo-misonidazole* (n = 5)	[^{3}H]-misonidazole* (n = 5)	[^{3}H]-fluoro-misonidazole† (n = 5)
Blood	2.77 ± 1.05	1.11 ± 0.29	0.73 ± 0.23	0.98 ± 0.07
Tumor	1.10 ± 0.19	3.36 ± 1.13	1.37 ± 0.45	1.29 ± 0.20
Brain	0.65 ± 0.36	1.02 ± 0.39	0.55 ± 0.11	0.88 ± 0.14
Liver	0.99 ± 0.53	2.48 ± 0.42	1.66 ± 0.38	4.49 ± 0.29
Kidney	1.60 ± 0.56	1.75 ± 0.58	1.44 ± 0.51	3.20 ± 0.54
Heart	0.82 ± 0.34	1.42 ± 0.60	0.90 ± 0.28	1.07 ± 0.15
Lung	1.76 ± 0.66	1.46 ± 0.74	0.97 ± 0.29	1.29 ± 0.18
Muscle	0.50 ± 0.27	0.94 ± 0.31	0.89 ± 0.33	0.91 ± 0.10

* BALB/c km mice.
† C3H/km mice.

and the blood levels at 2 hr were higher by a factor of 3. The blood clearance of [^{3}H]-fluoromisonidazole followed a course parallel to but below that of misonidazole at early times, but the values converged at 2 hr. The [^{82}Br]-4-bromomisonidazole/[^{3}H]-4-bromomisonidazole ratio in blood increased slowly over the first 2 hr, probably due to recirculation of a small amount of radioactive bromide ion.

The relatively high lipophilicity of 4-bromomisonidazole results in its rapid entry into cells. Distribution of [^{82}Br]-4-bromomisonidazole and [^{3}H]-4-bromomisonidazole between blood cells and plasma was measured at 15, 30, and 120 min after injection. This ratio increased over 30 min, reaching nearly equal proportions in cells and plasma. The label in the cells then slowly decreased relative to plasma over the next 2 hr.

The concentration of 4-bromomisonidazole in tissues at 2 hr after injection was measured by following both [^{82}Br] and [^{3}H] labels (Table 3). The ratio of the two labels, [^{82}Br]/[^{3}H], at 2 hr in most tissues was ≤1; the

exceptions were lung and blood where the values were 1.2 and 2.5, respectively. The tumor-to-organ ratio of [^{3}H]-4-bromomisonidazole at 2 hr showed a differential retention in tumor. Calculated tumor-to-organ ratios from 3.0 to 1.25 are in the range acceptable for tomographic imaging. Tumor-to-tissue ratios for [^{3}H]fluoromisonidazole at 2 hr were lower than those of [^{3}H] misonidazole, suggesting that the preferential retention by the tumor relative to normal tissues might be occurring at a later time for the fluorinated congener. [^{3}H]-4-Bromomisonidazole and its major metabolites in plasma, kidney, and liver were determined by HPLC at various times after injection and showed that the parent compound was present in considerable proportion at early times, but its amount declined over 30 min (Table 4). The concentration of ^{82}Br in plasma, kidney, and liver suggested some debromination occurs during 2 hr. When [^{3}H]-fluoromisonidazole was tested for stability in plasma, no detachment of the ^{3}H label was detected. The fluorinated drug is metabolized slowly, only 10%

TABLE 4
Misonidazole and Metabolites in Plasma and Tissues as Function of Time

Time after injection	DMM/BrDMM*	Misonidazole	Unknown†	4-bromomisonidazole	Unknown‡
Plasma					
15 min	27%	45%	—	28%	—
30 min	18%	40%	33%	8%	—
120 min	38%	62%	—	—	—
Liver					
30 min	31%	35%	—	16%	18%
120 min	84%	11%	—	7%	—
Kidney					
30 min	58%	21%	—	10%	11%
120 min	75%	14%	—	<2%	9%

* The peak eluted at 5 min contains both desmethylmisonidazole and 4-bromodesmethylmisonidazole, which were not resolved under conditions of the experiment.
† A product which eluted at 13 min was not identified.
‡ A product which eluted at 16–18 min was not identified.

of metabolized drug was detected in plasma by 30 min, 60% of 2 hr.

DISCUSSION

Detection and quantitation of tumor hypoxia noninvasively would be useful in patient evaluation prior to and during radiation therapy. An imaging agent for this assay is being designed based on hypoxic cell sensitizers. The requirements for such a tracer molecule are good penetration into cells, acceptable toxicity at the concentration to be administered, and stability of the label in vivo during the time needed for the imaging procedure. Important factors in choosing the label are half-life and ease of imaging. A positron emitting radiosensitizer labeled at high specific activity could lead to quantitative imaging of hypoxia.

The previous experience with misonidazole as a radiosensitizer in the radiotherapy clinic, its good localization and covalent binding in hypoxic tissues (23–25) and its low blood levels make it a compound of choice for a hypoxia imaging agent. Bromine-75 or bromine-77 and fluorine-18 are positron emitters with half-lives of 1.6, 56, and 1.8 hr, respectively, that have been suggested as likely radioactive labels for misonidazole congeners.

We synthesized compounds (III) and (V) and studied their feasibility as a bromine-labeled imaging agent of hypoxia. Bromination through the electrophilic brominating agent generated in situ (13) is the preferred synthetic route for radiobrominated (III). The yield by this route was higher (60%) and the product was easier to isolate, due to lower amounts of 5-bromo isomer. Radiobromide ion for synthesis can be obtained more conveniently and at higher specific activity than Br_2 and its conversion to an electrophilic brominating agent in situ results in higher radiochemical yields.

While the entry of the drug into tissue is a function of its partition coefficient, its retention during the washout phase depends on the presence of a hypoxic region. The concentration of radiosensitizer in normal tissues represents principally its solubility in aerobic cells. The high uptake into the liver is due to this organ's specific role in detoxification and its function as a major metabolic site, but possibly also due to hypoxia (18). The relatively higher uptake and retention in the tumor as compared to most other tissues including blood, is the most important parameter we have evaluated in searching for a hypoxic imaging drug. The necrotic regions of tumors show little uptake (8,10,25) because dead tissue cannot covalently bind misonidazole. The bromine atom on the imidazole ring makes the misonidazole molecule more lipophilic, and it thus crosses membranes faster. Bromination of misonidazole increased the partition coefficient sevenfold (Table 2). As a result, concentration of (III) and (V) in blood cells relative to

plasma at 15 min after injection was higher than for misonidazole.

The clinical use of radiosensitizers in radiation therapy is limited by normal tissue toxicity of the drug, principally peripheral neuropathy. Neural tissue toxicity is higher for drugs that are more lipophilic than misonidazole (3,26) and hence their use as imaging agents could be justified only if used as high specific activity tracers of hypoxia. The micromolar concentrations of misonidazole derivatives that give high tumor-to-normal tissue ratios are much lower than the millimolar quantities used for tumor radiosensitization.

The chemistry of misonidazole in vivo is complex. The parent drug is reduced to one or more products and other metabolites are formed, including demethylated forms. Some of these bind covalently to macromolecules (23,27,28). A major concern for an in vivo tracer is the stability of the label during these metabolic transformations. By following only the [^{82}Br]-tagged molecule we might be detecting a sum of parent compound, metabolites carrying the label, and free bromide ion following debromination. The ^{3}H label measures the total concentration of brominated parent and its brominated metabolites as well as [^{3}H]misonidazole, [^{3}H]desmethylmisonidazole and other [^{3}H]-labeled metabolites obtained by debromination. Clearance of the two compounds from the blood was similar at 5 min after injection, but then the slope of the tritium curve increased gradually and at 2 hr assumed the level of misonidazole (Fig. 2). The two-label experiments using [^{82}Br]/[^{3}H] were designed to test the stability of the two labels in vivo and their metabolic equivalence. [^{82}Br]-4-bromomisonidazole behaved in vivo somewhat differently from [^{3}H]-4-bromomisonidazole. Increase of the ratio [^{82}Br]/[^{3}H] in the blood over 2 hr is consistent with loss of bromine and is evident from the blood clearance data (Fig. 2). This debromination caused a blood level of ≥2.5% ID/g at 2 hr after injection, which is too high a background for imaging.

Hydrogen-3-fluoromisonidazole was tested using the same criteria. The lipophilicity of fluoromisonidazole is comparable to misonidazole, but the uptake into the tumor and tumor-to-tissue ratios at 2 hr were lower, indicating that its entry into tissues was slower (Table 3). This compound has been labeled with ^{18}F previously (29) and the fluorine label has been shown to be stable in vivo in plasma. These results suggest that longer diffusion times might be required to achieve acceptable target/background ratios for imaging. This is in contrast to 4-bromomisonidazole which enters tissues faster than misonidazole and achieves imagable tumor-to-tissue ratios before substantial loss of label occurs. However, the bond between bromine and the imidazole ring comes apart, either hydrolytically or by some metabolic reaction involving the ring, resulting in excessive radioactive bromide ion background at an otherwise ideal

imaging time. These results suggest that one might obtain a superior radiopharmaceutical by modifying [^{18}F]fluoromisonidazole through the addition of a non-radioactive 4-bromo substituent. The bromine would increase lipophilicity and hence rate of transport of the molecule into the tissues. The radioactive fluorine would provide a stable, nonmetabolized label for imaging. The bromine would stay attached long enough to achieve optimal pharmacokinetics and, even though some bromine would separate from the misonidazole, the nonradioactive bromine would not interfere with imaging. Of other ring substituents that would increase the partition coefficient of the fluoromisonidazole, perhaps a 4-methyl substituent would be the most attractive. It might give the same effect observed for the 4-bromo derivative without the concern for in vivo metabolism. Such considerations will be further evaluated in our continued studies with tracer compounds.

NOTES

ACKNOWLEDGMENTS

REFERENCES

1. Chapman JD, Raleigh JE, Pederson JE, et al. Potentially three distinct uses for hypoxic cell sensitizers in the clinic. In: Okada S, Imamura M, Terashima T, et al., eds. Proc VI Int Congress Radiat Res 1979; 885–893.
2. Workman P. Pharmacokinetics of hypoxic cell radiosensitizers. A review. Cancer Clin Trials 1980; 3:237–251.
3. Brown JM, Workman P. Partition coefficient as a guide to the development of radiosensitizers which are less toxic than misonidazole. Radiat Res 1980; 82:171–190.
4. White RAS, Workman P, Brown JM. The pharmacokinetics and tumor and neural tissue penetrating properties of SR-2508 and SR-2555 in the dog—hydrophilic radiosensitizers potentially less toxic than misonidazole. Radiat Res 1980; 84:542–561.
5. Chapman JD, Franklin AJ, Sharplin J. A marker for hypoxic cells in tumors with potential clinical applicability. Br J Cancer 1981; 43:546–558.
6. Rasey JS, Krohn KA, Freauff S. Bromomisonidazole: synthesis and characterization of a new radiosensitizer. Radiat Res 1982; 91:542–554.
7. Rasey JS, Grunbaum Z, Krohn KA, et al. Comparison of binding of [^{3}H]misonidazole and [^{14}C]misonidazole in multicell spheroids. Rad Res 1985a; 101:473–479.
8. Garecht BM and Chapman JD. The labeling of EMT-6 tumors in BALB/c mice with ^{14}C-misonidazole. Br J Radiol 1983; 56:745–753.
9. Rasey JS, Krohn KA, Grunbaum Z, et al. Further characterization of 4-bromomisonidazole as a potential detector of hypoxic cells. Radiat Res 1985b; 102:76–85.
10. Chapman JD, Baer K, Lee J. Characteristics of the metabolism-induced binding of misonidazole to hypoxic mammalian cells. Cancer Res 1983; 43:1523–1528.
11. Hoffman JM, Rasey JS, Spence AM, et al. Binding of the hypoxia tracer ^{3}H-misonidazole in cerebral ischemia. Stroke: in press.
12. Fujita T, Iwasa J, Hansch C. A new substituent constant, Pie, derived from partition coefficients. J Am Chem Soc 1964; 86:5175–5180.
13. Wilbur DS, Anderson KW. Bromine chloride from N-chlorosuccinimide oxidation of bromide ion. Electrophilic addition reactions in protic and aprotic solvents. J Org Chem 1983; 47:1542–1544.
14. Born JL, Smith BR. The synthesis of tritium labeled misonidazole. J Label Comp 1983; 20:429–432.
15. Beaman AG, Tautz W, Duschinsky R. Antimicrob Agents Chemother 1967; 520–530.
16. Rasey JS, Carpenter RE, Nelson NJ. Response of EMT-6 tumors to single fractions of x-rays and cyclotron neutrons. Radiat Res 1977; 71:430–446.
17. Rasey JS, Krohn KA, Menard TW, et al. Comparative biodistribution and radioprotection with three radioprotective drugs in mouse tumors. Int J Radiat Oncol Biol Phys: in press.
18. Flockhart IR, Large P, Troup SL, et al: Pharmacokinetics and metabolic studies of the hypoxic cell radiosensitizer misonidazole. Xenobiotica 1978; 8:97–105.
19. Moulder JE, Rockwell S. Hypoxic fractions of solid tumors: experimental techniques, methods of analysis, and a survey of existing data. Int J Radiat Oncol Biol Phys 1984; 10:695–712.
20. Harper HA: Review of physiological chemistry. Los Altos, CA: Lange Medical Publications, 1973: 185.
21. Hubbard RW, Beierle FA. Sample preparation and a liquid chromatographic assay for misonidazole. J Chrom 1982; 232:443–449.
22. Wong TW, Whitmore GF, Gulyas S. Studies on the toxicity and radiosensitizing ability of misonidazole under condition of prolonged incubation. Radiat Res 1978; 75:541–555.
23. Varghese AJ, Whitmore GF. Binding to cellular macromolecules as a possible mechanism for the cytotox-

icity of misonidazole. *Cancer Res* 1980; 40:2165–2169.

24. Van Os-Corby DJ, Chapman JD. In vitro binding of ^{14}C-misonidazole to hepatocytes and hepatoma cells. *Int J Radiat Oncol Biol Phys*: in press.

25. Horowitz M, Blasberg R, Molnar P, et al. Regional [^{14}C]misonidazole distribution in experimental RT-9 brain tumors. *Cancer Res* 1983; 43:3800–3807.

26. Clarke C, Dawson KB, Sheldon PW, et al. Neurotoxicity of radiation sensitizers in the mouse. *Int J Radiat*

Oncol Biol Phys 1982; 8:787–789.

27. Varghese AJ, Whitmore GF. Cellular and chemical reduction products of misonidazole. *Chem Biol Interactions* 1981; 36:141–151.

28. Rauth AM. Pharmacology and toxicology of sensitizers: mechanism studies. *Int J Radiat Oncol Biol Phys* 1984; 10:1293–1300.

29. Jerabek PA, Dishino DD, Kilbourn MR, et al. Synthesis of a fluorine-18 labeled hypoxic cell sensitizer [Abstract]. *J Nucl Med* 1984; 25:P23.